ChemPubSoc Europe

DOI: 10.1002/celc.201300055

Realization of an Artificial Three-Phase Reaction Zone in a Li–Air Battery

Moran Balaish,[a] Alexander Kraytsberg,[b] and Yair Ein-Eli*[a, b]

Metal–air batteries provide electricity through a redox reaction between a metal anode and ambient oxygen (which does not have to be stored in the system, but can be accessed from the environment). Such batteries are promising power sources with a theoretical high specific energy.[1–3] Amongst various metals, there are good reasons to place more emphasis on the development of lithium–air systems, particularly due to the system's outstanding specific capacity (3842 mAh per 1 g of lithium vs. 815 mAh per 1 g of zinc). Lithium undergoes severe corrosion in aqueous electrolytes;[4] thus, a practical and viable Li–air cell design should be based on the implementation of non-aqueous electrolytes.[5] As a matter of fact, most current Li–air systems are comprised of a Li-metal anode, a non-aqueous electrolyte, and a porous air-breathing cathode; commonly, the cathode is comprised of catalyst-coated carbon particles with a large surface area. The air electrode promotes intimate contact of the electrode material with the solution and gaseous phase, compensating for the low intrinsic rate of the heterogeneous electrochemical reaction by providing a large interfacial area per volume unit.[6] Non-aqueous electrolytes present a significant challenge to the operation of air cathodes. With aqueous electrolytes, a three-phase system is formed in the air cathode, comprised of two interpenetrating sub-systems of hydrophobic and hydrophilic micro-channels (pores).The two sub-systems are interconnected; oxygen diffuses through gas-filled hydrophobic pores while hydrophilic pores transport metal-ions to and from the reaction sites, enabling the oxygen reduction reaction (ORR) to occur at three-phase boundary reaction zones.[7] Flooding of the gas-filled pores is undesirable as it decreases oxygen accessibility at the cathode reaction centers, resulting in reduced current density. However, most organic electrolytes easily wet all electrode pores while flooding air channels, and hence only dissolved O_2 participates in the actual ORR charge-transfer reaction, occurring in a two-phase boundary reaction zone.[7] Schemes 1a and 1b illustrate the pathways of ORR taking place at the oxygen cathode in such cases. As a result, oxygen availability is determined by the level of its dissolution and diffusion in the electrolyte, making these parameters crucial in determining the overall air cathode performance. A particular aspect worth consideration is the low mobility of dissolved oxygen; in a dissolved form, it is substantially less mobile compared to gaseous oxygen by at least one order of magnitude.[8–10] A substantial O_2-concentration gradient is being formed along the pores during cell discharge, and as a result, Li oxides predominantly precipitate in the vicinity of the pore orifices, eventually clogging them.[11] This feature is highlighted by the reported enhancement in air cathode performance under increased oxygen pressure. Namely, if the oxygen pressure is increased from 0.2 (air) to 2 atm. at a discharge current of 0.05 mA cm^{-2}, the specific capacity increases tenfold.[8] Apparently, increased oxygen pressure results in both higher oxygen solubility and concentration in the electrolyte solution, resulting in an increased specific capacity. It is hypothesized that higher O_2 pressure compels dewetting of some cathode pores, forcing the formation of desirable 3-phase reaction zones throughout the air electrode (similar to air cathodes in contact with aqueous electrolyte).[12] In short, the abilities of non-aqueous electrolytes to both dissolve and transport oxygen are crucial parameters determining both the energy and power capacities of the cell.[13,14] Although many common non-aqueous electrolytes provide adequate conductivity, wide stability windows and even compatibility with lithium anodes, they all possess low O_2-solubility, poor oxygen diffusivity and also are often prone to water vapor absorption.[15–17]

A promising way to increase oxygen mobility in Li–air system is through the preparation of an artificial three-phase boundary (Scheme 1c) by employing an electrolyte comprising

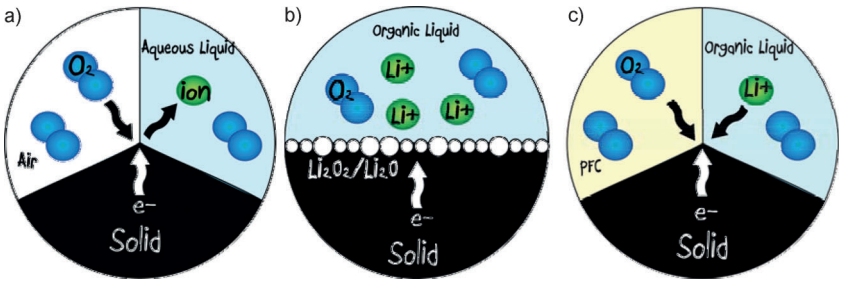

Scheme 1. Models of reaction zones for electrochemical oxygen reduction: a) a "three-phase reaction zone" for aqueous electrolytes; b) a "two-phase" reaction zone for non-aqueous electrolytes;[5] and c) an artificially fabricated "three-phase reaction zone" for non-aqueous electrolyte Li–air battery.

[a] M. Balaish, Prof. Y. Ein-Eli
The Grand Technion Energy Program
Technion- Israel Institute of Technology
Haifa 32000 (Israel)

[b] Dr. A. Kraytsberg, Prof. Y. Ein-Eli
Department of Materials Science and Engineering
Technion- Israel Institute of Technology
Haifa 32000 (Israel)
Fax: (+972) 77-8871977
E-mail: eineli@technion.ac.il

Supporting information for this article is available on the WWW under http://dx.doi.org/10.1002/celc.201300055.

two immiscible components (marked in yellow and blue in Scheme 1 c). One of the components (marked in yellow) has outstanding oxygen transport ability, and another component is a non-aqueous polar liquid with Li^+ transport ability. Partial impregnation of the cathode with the first electrolyte component, is expected to secure oxygen transport to the catalytically active cathode sites, where charge transfer occurs. The aqueous electrolyte component: The role of the latter would be to secure ionic conductivity between cell electrodes, and to transport Li^+ ions to the cathode reaction sites. Good component candidates are perfluorinated carbon liquids (PFCs). PFC solvents have long been known to be media with fast oxygen dissolution kinetics and high oxygen solubility.[18–20]

Fluorocarbons and their derivatives are also well-known for their thermal stability, chemical and electrochemical inertness.[21] The last is advantageous as the environment of Li–air cells is highly oxidative. Some of their distinct properties are: lower boiling points than corresponding carbohydrates, extreme hydrophobicity, substantial lipo-phobicity and the ability to dissolve large quantities of gases (especially oxygen) (see Table S1 of the Supporting Information, SI).[22–27] Oxygen solubility in perfluorocarbons is 3–10 times higher than the value observed for parent hydrocarbons or in water, respectively.[20,28] Additionally, the O_2 diffusion coefficients in PFCs are, in general, twice as large as those observed in water.[27] Due to their low polarity, perfluoro solvents are immiscible polar electrolyte solvents.[29,30] In the suggested structure design, PFCs are expected to provide continuous channels for oxygen transport inside cathode pores while facilitating Li-oxide deposition throughout the whole cathode volume and preventing premature pore clogging, allowing higher utilization of pores for Li-oxide filling. On the other hand, PFCs should be introduced in such a way that it would fill only a certain portion of the cathode pores, leaving enough room for channels to be filled with the Li^+-conducting electrolyte component; these channels are to offer a continuous path for Li^+—transport to the cathode reaction sites.

Four different perfluorinated additives; PFO, PF1, PF2 and PF3 (see Experimental Section) were chosen in the present work. According to the above deliberation, it is not enough just to fill the cell with mixed electrolyte (O_2-transporting component and Li^+-transferring component),[21] there is a need to form a nanoscale regular structure comprising of two interconnected channel subsystems inside the air cathode. Apparently, PFCs should be immiscible in the organic electrolyte to be permanently located inside the air electrode pores rather than to migrate from the pores into the organic electrolyte. The miscibility of a common Li–air electrolyte, namely, triethylene glycol dimethyl ether (TEGDME) and fluorinated carbon compounds (such as PF0) was examined and found to be 0.10% vol (see SI). The commercially available air cathode was heated to remove water from the carbon pores, then a small drop (0.05 mL) of PFC was placed at the carbon cathode surface; the PFC was readily absorbed into the cathode structure. To achieve full impregnation of the cathode *meso*-pores by the PFC, the modified air electrode was kept in vacuum overnight at room temperature. The effect of PFC treatment was examined in an electrochemical cell containing a 1 M $LiPF_6$ dissolved in a.[31,32] Figure 2 a presents discharge curves obtained from Li–air cells utilizing different PFC-modified air cathodes. Overall, the results demonstrate that cathode treatment with PFC presents superior performance—it substantially increased the cathode discharge capacity by 60% and improves Li–air discharge voltage. To demonstrate that Li_2O_2 is the predominant discharge product, Raman spectroscopy was conducted after discharge for both the PFC-modified and pristine cathodes (Figure S2). It is worth mentioning that the specific discharge capacity was calculated in mAh g^{-1}, where the mass of carbon in the air electrode was used for the calculations. The concern of using the carbon mass for specific capacity calculations arises from the variation of carbon loading, making it a rather problematic comparison parameter. Indeed, studies based on a low carbon loading can provide a high discharge capacity based on the carbon mass. Beattie et al.[33] reported a discharge capacity in the Li–air system of 6000 mAh g^{-1} when carbon loading was as low as 2 mg cm^{-2}, while the discharge capacity decreased to 250 mAh g^{-1} at a carbon loading of 6 mg cm^{-2}. The commercial air electrode in the present study has a carbon loading of 19 mg cm^{-2}.

Figure 1 b demonstrates the influence of the current density on Li–air cells utilizing PFC-treated cathodes. Although it was anticipated that PFC treatment would lead to a substantial voltage gain, no effect was observed when the current was increased fivefold (from 0.1 to 0.5 mA cm^{-2}). Such behavior may be assigned to phenomena related to the ORR rate, determined by different discharge currents. At higher currents such as 0.5 mA cm^{-2}, the low discharge capacity attained in spite of the pores being only sparsely packed with fine discharge products (Figure S3B), can only be reconciled with a mechanism controlled by diffusion. Low oxygen mobility in the organic electrolyte may suppress high-rate ORR, leading to a higher discharge over-potential and a premature voltage drop. Thus, even when PFC is employed, only a relatively small capacity increase (12.7%) is observed. When lower currents such as 0.1 or 0.2 mA cm^{-2} are applied, densely packed coarser particles are formed (figures S3C and S3D, respectively), enabling further capacity increase after PFC addition (33.8% and 42.8%, respectively). In these cases it is possible that the mechanism responsible for the premature voltage drops is controlled by the formation of insoluble and nonconductive discharge products. It appears that for this PFC modified air electrode a current density of 0.2 mA cm^{-2} is an ideal one in terms of capacity and discharge over-voltage improvement. It was determined that the PFC (PF1) absorbance capacity in the air electrode was limited to 10 μl PF1 (after vacuum treatment) even when 20, 50, 100 and 200 μL of PF1 were added to the electrode (see SI, Figure S1). Since the amount of oxygen that could have been introduced in 10 μl PF1 is approximately three orders of magnitude lower than the amount of oxygen consumed throughout the discharge process, it is clear that the PFC–air cathode modification resulted in the formation of hydrophobic channels that facilitate oxygen transport, and that the air cathode pores were not subjected to flooding by the organic solution.

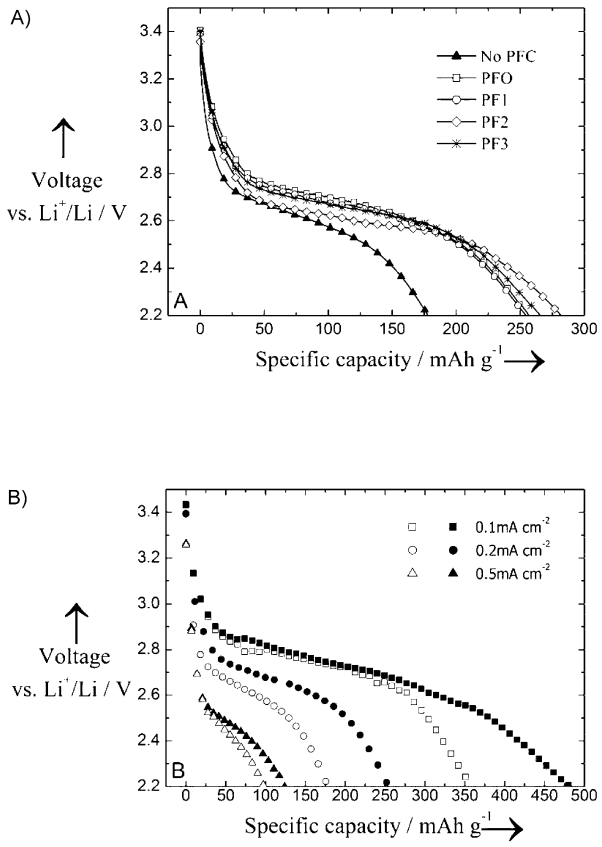

Figure 1. Discharge curves of Li–air cells in 1 M $LiPF_6$ /TEGDME: A) with PFO (squares), PF1 (circles), PF2 (rhombus), PF3 (asterisks) and without PFC (triangles) at 0.2 mA cm^{-2}; B) with (bold) and without PF1 at 0.5 mA cm^{-2} (triangles), 0.2 mA cm^{-2} (circles) and 0.1 mA cm^{-2} (squares).

A deeper understanding of the mechanism behind the complex PFC/air cathode system is gained by performing potentiostatic measurements. Figure 2 presents a comparison potentiostatic curves obtained from Li–air cells utilizing modified PF1 and pristine air electrode at 2.6 V vs. Li^+/Li in 1 M $LiPF_6$/TEGDME solution. After assembling the two cells inside the glove box, they were kept in an ambient environment for 24 h to ensure oxygen diffusion into the cell. At the next stage, the cell air openings were sealed and potentiostatic experiments were conducted at 2.6 V vs. Li^+/Li. No meaningful difference in current values for both the treated and untreated air electrodes was found (potentiostatic experiments conducted at 2.7 V vs. Li^+/Li showed no difference either). These results support the assumption that the observed improvement in cell discharge capacity via the addition of PFC is not due to higher oxygen concentration, but rather through a modification of the air electrode pore structure.

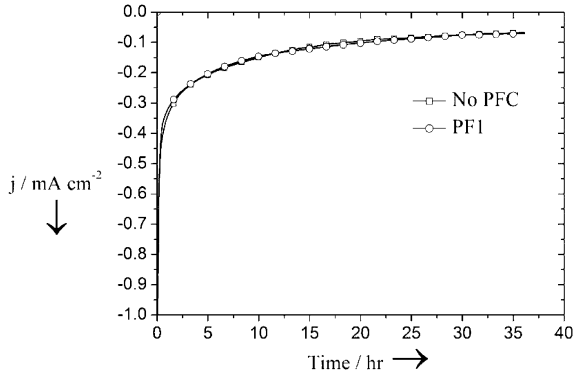

Figure 2. Potentiostatic curves of Li–air cells with PF1 (○) and without (□) at 2.6 V vs. Li^+/Li in 1 M $LiPF_6$/ TEGDME. The cells were held in an ambient environment for 24 h prior to activation.

Figure 3 presents high-resolution scanning electron microscopy (HRSEM) images of the air side and the electrolyte-facing side of the air cathodes for the pristine and discharged Li–air cells with and without PF1 addition. The individual carbon particles of the pristine electrode have primary sizes on the order of 50 nm (Figure 3 a). Spheres with a diameter of 200–300 nm were observed at the air side for the non-PFC treated electrode after discharge at 0.2 mA cm^{-2}(Figure 3 b). Yet, no products were observed at the electrode side facing the solution (Figure 3 e).

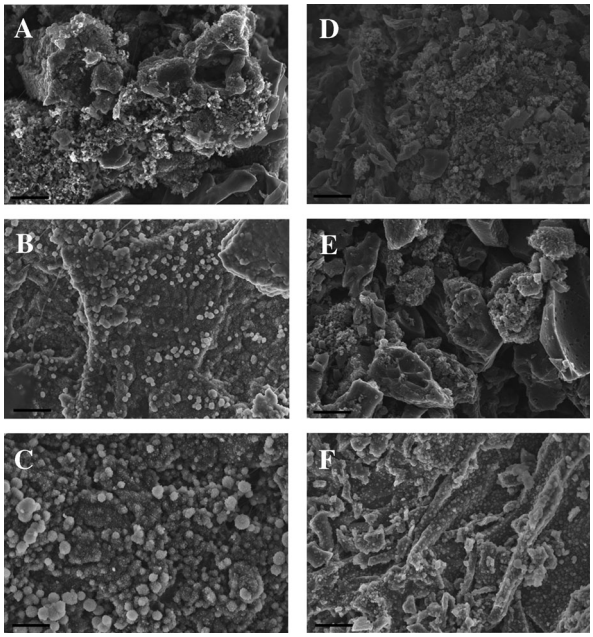

Figure 3. HRSEM micrographs obtained from the air side of: A) a pristine air electrode; B) an air electrode after discharge at 0.2 mA cm^{-2}; and C) a PF1-modified air electrode after discharge at 0.2 mA cm^{-2}; and from the solution-facing side of: D) a pristine air electrode; E) an air electrode after discharge at 0.2 mA cm^{-2}; and F) a PF1-modified air electrode after discharge at 0.2 mA cm^{-2} (the scale bars are 2 μm).

Spheres were observed both at the air side as well as at the solution side of the cathode in the PFC-modified air electrode (Figure 3 c and Figure 3 f, respectively). Larger particles were formed at the PFC-modified air electrode compared with the non-treated electrode. Thus, the HRSEM micrographs support the notion that PFCs form oxygen transportation channels inside the cathode pores, facilitating wider oxygen distribution in the cathode volume while making a larger share of the same volume available for Li–oxide filling. Figures 3 e and Fig-

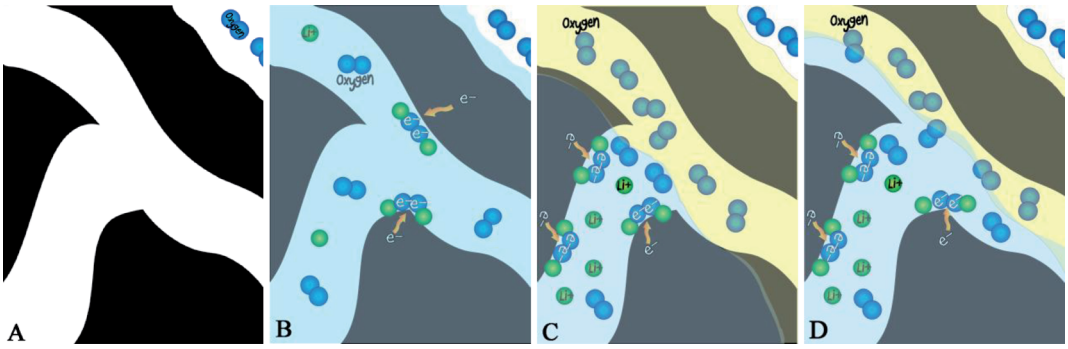

Scheme 2. Illustration of the proposed mechanism realizing the formation of an artificial three-phase reaction zone in Li–air cathode: A) Channels inside the pristine porous carbon; B) channels are flooded with an organic electrolyte (in blue) thus, only dissolved oxygen is participating in the reduction reaction; C–D) different possibilities of two distinct subsystem channels, G_{PFC} (in yellow) and G_{Li-ion}, formed as a result of the PFC treatment.

ure 3 f, which present micrographs of the solution-facing side of the air cathode subsequent to a 0.2 mA cm^{-2} discharge for the untreated and PF1-treated air cathodes, provide further support for the outlined improvement mechanism: although no discharge products were observed in the untreated air cathode, the volume and surface of PF1-treated cathode was better exploited. This observation can explain the enhancement in cell capacity.

Summarizing all the above, the air cathode structure (marked as $G_{cathode}$) may be presented as being comprised of two distinct subsystem channels, G_{PFC} and G_{Li-ion} [Eq. (1)]:

$$G_{cathode} = G_{PFC} \cup G_{Li-ion} \quad (1)$$

G_{PFC} is wetted with PFC and provides oxygen transport paths, whereas G_{Li-ion} is filled with electrolyte and provides Li^+-transport paths. As illustrated in Scheme 2, the edges of G_{PFC} connect the cathode air side to catalytically active cathode centers, and the edges of G_{Li-ion} connect these centers to the bulk of the cell electrolyte. Each center is a vertex of both G_{Li-ion} and G_{PFC} (i.e., each catalytic center is to be supplied with both O_2 and Li^+), making G_{Li-ion} and G_{PFC} complementary subsystems. Vertices that are not located at the G_{PFC}/G_{Li-ion} interface are less involved in charge transfer due to substantially lower oxygen concentration, and thus pores which house such vertices experience less Li-oxide filling. It may be suggested that the most efficient PFC-treatment would lead to an optimal $G_{cathode}$, having a maximal amount of charge-transfer centers in the air cathode.

In summary, a new approach for designing cathodes with high oxygen-transport properties for non-aqueous Li–air cells is presented. The essence of the new design is the formation of two interpenetrating network channels; one network consists of channels filled with O_2-transporting PFCs and the other is filled with a Li^+-conducting electrolyte. These systems become components of a three-phase reaction zone inside the air cathode. Our results demonstrate that the PFC-treatment substantially increases the cathode discharge capacity and improves Li–air cell voltage. The observed cathode-capacity enhancement and increased discharge voltage for treated cathodes confirm the assumption of the major impact of increased oxygen transport in the Li–air cathode. The particular structure and design of these networks are suggested to be the prime feature for determining the properties of PFC-treated air cathodes. Our current work is focusing on the rechargeability of the Li–air/PFC system and will be reported in the future.

Experimental Section

A high-surface-area commercial air electrode composed of a MnO_2 catalyst dispersed in activated carbon powder (carbon loading 19 mg cm^{-2}) was purchased from Electric Fuel, Inc (see SI, Figure S5). The cathode was heated overnight at 100 °C under vacuum to remove all the water from the carbon pore system. Then, a small drop (0.05 mL) of PFC was placed on the carbon side of the cathode surface and was kept in vacuum overnight (100 mbar) at room temperature. Different perfluorocarbons were examined. Perfluoro-n-octane (98%) (PFO), perfluoro (decahydrophtalene) (cis/trans, 95%) (PF1),1-bromoperfluoroheptane (97%) (PF3) and perfluoro-n-nonane (99%) (PF2) were purchased from Alfa Aesar and were used as received.

A Li–air lab-scale battery with a three-electrode configuration was designed and manufactured (see SI, Figure S4). All experiments were conducted in a four-liter sealed chamber with approximately 15% relative humidity (RH) achieved by using calcium chloride salt as a desiccant. The electrolyte was a solution of 1 M LiPF6 in triethylene glycol dimethyl ether (TEGDME, 99%, Alfa Aesar). The solvent was dried with 3 Å molecular sieves (8–12 mesh, Sigma–Aldrich) for four days. The moisture content in the solvent was measured with a Karl Fisher titrator (Metrohm 831 KF coulometer), and determined to be less than 50 ppm water before use. All electrolytes were prepared inside an inert glove box (H_2O, $O_2 < 5$ ppm).

Electrochemical Measurements

Discharge experiments were carried out with a battery cycler (Arbin Instruments, BT2000). All cells were held at OCP (open circuit potential) for 12 h prior to discharge initiation. Potentiostatic studies were performed with an EG&G Princeton Applied Research potentiostat/galvanostat 2273.

Characterization Method

The surface morphology of the air cathode was studied using a high-resolution scanning electron microscope (HRSEM, Zeiss Ultra-Plus FEG-SEM).

Acknowledgements

The authors acknowledge the support from the Grand Technion Energy Program (GTEP), Israel National Research for Electrochemical Propulsion (INREP), FP7 InnoEnergy Program, the Helmsley Charity Fund and the Israeli Ministry of Energy and Water Resources.

Keywords: lithium–air batteries · oxygen · perfluorocarbon · power sources · three-phase reaction zone

[1] J. S. Lee, S. Tai Kim, R. Cao, N. S. Choi, M. Liu, K. T. Lee, J. Cho, *Adv. En. Mat.* **2011**, *1*, 34 – 50.
[2] M. Armand, J. Tarascon, *Nature* **2008**, *451*, 652 – 657.
[3] A. Kraytsberg, Y. Ein-Eli, *J. Power Sources* **2010**, *196*, 886 – 893.
[4] A. Galbraith, *International Electric Vehicle Symposium*, **1976**.
[5] K. Abraham, Z. Jiang, *J. Electrochem. Soc.* **1996**, *143*, 1 – 5.
[6] J. Newman, W. Tiedemann, *AIChE J.* **2004**, *21*, 25 – 41.
[7] S. S. Zhang, D. Foster, J. Read, *J. Power Sources* **2010**, *195*, 1235 – 1240.
[8] J. Read, K. Mutolo, M. Ervin, W. Behl, J. Wolfenstine, A. Driedger, D. Foster, *J. Electrochem. Soc.* **2003**, *150*, A1351.
[9] D. R. Lide, *CRC Handbook of Chemistry and Physics*, CRC Press/Taylor and Francis, Boca Raton, FL, **2010**.
[10] Mark W. Denny, *Air and Water: The Biology Adn Physics of Life's Media*, Princeton University Press, New Jersey, U.S.A, **1993**, p. 341.
[11] C. Tran, X. Q. Yang, D. Qu, *J. Power Sources* **2010**, *195*, 2057 – 2063.
[12] J. Christensen, P. Albertus, R. S. Sanchez-Carrera, T. Lohmann, B. Kozinsky, R. Liedtke, J. Ahmed, A. Kojic, *J. Electrochem. Soc.* **2012**, *159*, R1.
[13] I. Kowalczk, J. Read, M. Salomon, *Pure Appl. Chem.* **2007**, *79*, 851 – 860.
[14] R. Padbury, X. Zhang, *J. Power Sources* **2011**, *196*, 4436 – 4444.
[15] W. Xu, J. Xiao, J. Zhang, D. Wang, J. G. Zhang, *J. Electrochem. Soc.* **2009**, *156*, A773.
[16] C. O. Laoire, S. Mukerjee, K. Abraham, E. J. Plichta, M. A. Hendrickson, *J. Phys. Chem. C* **2010**, *114*, 9178 – 9186.
[17] W. Xu, J. Xiao, D. Wang, J. Zhang, J. G. Zhang, *J. Electrochem. Soc.* **2010**, *157*, A219.
[18] L. C. Clark Jr, F. Gollan, *Science* **1966**, *152*, 1755.
[19] M. Costa Gomes, J. Deschamps, D. H. Menz, *J. Fluorine Chem.* **2004**, *125*, 1325 – 1329.
[20] J. Deschamps, M. F. Costa Gomes, A. A. H. Pádua, *J. Fluorine Chem.* **2004**, *125*, 409 – 413.
[21] Y. Wang, D. Zheng, X. Q. Yang, D. Qu, *Energy Environ. Sci.* **2011**, *4*, 3697 – 3702.
[22] A. M. A. Dias, R. P. Bonifácio, I. M. Marrucho, A. A. H. Pádua, M. F. Costa Gomes, *Phys. Chem. Chem. Phys.* **2003**, *5*, 543 – 549.
[23] A. M. A. Dias, M. Freire, J. A. P. Coutinho, I. M. Marrucho, *Fluid Phase Equilib.* **2004**, *222 – 223*, 325 – 330.
[24] A. M. A. Dias, C. M. B. Gonçalves, J. L. Legido, J. A. P. Coutinho, I. M. Marrucho, *Fluid Phase Equilib.* **2005**, *238*, 7 – 12.
[25] D. M. Lemal, *J. Org. Chem.* **2004**, *69*, 1 – 11.
[26] R. Navari, W. Rosenblum, H. Kontos, J. Patterson, *Res. Exp. Med.* **1977**, *170*, 169 – 180.
[27] M. K. Tham, R. D. Walker Jr, J. H. Modell, *J. Chem. Eng. Data* **1973**, *18*, 411 – 412.
[28] M. H. A. Hamza, G. Serratrice, M. J. Stebe, J. J. Delpuech, *J. Am. Chem. Soc.* **1981**, *103*, 3733 – 3738.
[29] P. Babiak, A. Němcová, L. RulíŠek, P. Beier, *J. Fluorine Chem.* **2008**, *129*, 397 – 401.
[30] A. M. A. Dias, C. M. B. Gonçalves, I. Ana, L. M. Santos, M. M. Piñeiro, L. F. Vega, J. A. P. Coutinho, I. M. Marrucho, *J. Chem. Eng. Data* **2005**, *50*, 1328 – 1333.
[31] S. A. Freunberger, Y. Chen, N. E. Drewett, L. J. Hardwick, F. Bardé, P. G. Bruce, *Angew. Chem.* **2011**, *123*, 8768 – 8772; *Angew. Chem. Int. Ed.* **2011**, *50*, 8609 – 8613.
[32] C. Ó. Laoire, S. Mukerjee, E. J. Plichta, M. A. Hendrickson, K. Abraham, *J. Electrochem. Soc.* **2011**, *158*, A302 – A308.
[33] S. D. Beattie, D. M. Manolescu, S. L. Blair, *J. Electrochem. Soc.* **2009**, *156*, A44 – A47.

Received: May 23, 2013
Published online on July 1, 2013